FINAL REPORT

JPL Contract Number 953161

Molecular-Beam Gas-Sampling System

Prepared by

W. S. Young and E. L. Knuth
December 1972
Molecular-Beam Laboratory
Energy and Kinetics Department
School of Engineering and Applied Science
University of California, Los Angeles
Los Angeles, California 90024

CONTENTS

ABSTRACT

I. INTRODUCTION

II. DESIGN PARAMETERS

A. Problems Associated with Rocket Samplings

B. Equation for Gases Flowing Through a Sonic Nozzle

C. Equation for Gases Flowing Through a Pumping System

D. Free-Jet Parameters

E. Pumping Load for a Collimating Chamber

F. Summary

III. SYSTEM DESCRIPTION

A. The Vacuum System

B. The End Plate

C. The Rocket Engine Mounting Plate

D. The Heat-Shield Assembly

E. The Skimmer Assembly

F. The Beam Detector

IV. EXPERIMENTAL RESULTS

A. Cooling-Water Flow Rate

B. Spacing Between the End Plate and the Sampling Nozzle

C. Sampling Capability

ACKNOWLEDGMENTS

REFERENCES

I

ABSTRACT

This report describes the molecular-beam mass-spectrometer system for rocket-motor combustion-chamber sampling designed for the Jet Propulsion Laboratory, Pasadena, California, by the Molecular-Beam Laboratory, University of California, Los Angeles, California under Contract No. 953161.

In Chapter I, the present studies are motivated, and the history of the sampling system is reviewed. Chapter II describes the problems associated with rocket-motor combustion-chamber sampling. Several design equations are presented.

The essential system components are described briefly in Chapter III. In liew of detailed drawings in the text, on-file JPL Drawing Numbers are cited.

In Chapter IV, the experimental results are presented. These results include cooling-water flow rates, the optimum separation gap between the end plate and the sampling nozzle, and preliminary data on compositions in a rocket-motor combustion chamber. Several finished and unfinished problems are discussed in Chapter V.

I. INTRODUCTION

The unlike doublet injector system commonly used in liquid rocket engines is intended to produce a spray of well-mixed droplets of fuel and oxidizer. The spray and mixing process is complicated and has been studied by numerous rocket scientists [1-3]. Recent evidence has shown that a strong exothermic reaction in the impinging region causes the injected streams to blow apart before substantial mixing can occur and results in poor combustion efficiency as well as a destructive combustion instability called popping. Operational engines in which popping was identified or suspected during development include the Titan/Gemini launch engines, the Apollo service propulsion engine, and the Transtage engine. Therefore, detailed studies for further understanding of the combustion process and better rocket injector design criteria are motivated.

Although the water-cooled sampling probe [3] is capable of sampling the gases in the rocket combustion chamber, some disadvantages of this sampling technique remain to be overcome. Firstly, the relatively long response time (3 seconds) of the sampling time compared with the allowable rocket testing time (5 to 6 seconds) prohibits the mass spectrometer from operating under slow sweep rate and results in a relatively poor mass resolution. Secondly, some reactive species were not detected due to their reactions with or absorptions by the sampling line wall. Furthermore, the signals obtained are time-averaged and hence do not represent the time-dependent propellant distribution realized with unstable combustion. Any new instrument seeking to replace this probe has to meet the following specifications: (a) its response time must be much shorter than the test time, (b) it must monitor at least most of the chemical species,

including some reactive ones, (c) it must function in high-temperature, high-pressure, and corrosive environments, and (d) it must preserve the (nonequilibrium) thermodynamic state of the combustion field.

Although various types of instruments have been developed for gas sampling, recent studies have shown that a supersonic molecular beam mass spectrometer sampling system satisfies the above listed requirements with best balance. Several investigators [4-8] have developed molecular-beam mass-spectrometer systems for high-pressure high-temperature gas samplings. Figure 1 shows the application of such a system in sampling from a rocket-motor combustion chamber. The combustion gas expands via the sampling orifice located at the tip of the heat-shield into the first vacuum stage (the source chamber). The skimmer transfers the core of the free jet into the second vacuum stage (the collimating chamber). The molecules flying near the system centerline then pass through the collimator and form a molecular beam. The mass spectrometer intercepts and ionizes the beam molecules to obtain a signal proportional to the beam density.

The success of a molecular beam system relies largely on the rapid quenching of rate processes during the free jet expansion. In Fig. 2, Knuth [9] plotted the temperature ratio T/T_o as a function of the dimensionless parameter $a_o t/d^*$. Here T is temperature, a is sound speed, t is flow time (zero at the throat), d* is throat diameter, and subscript o refers to source (stagnation) conditions. For a_o = 1000 m/sec and d* = 0.1 mm, a unit increase in $a_o t/d^*$ (and a major reduction in T/T_o) is realized in only 10^{-7} sec. Recently, Young et al. [10] developed a molecular beam mass spectrometer system for direct sampling of combustion gases inside an internal combustion engine. Their sampling system demonstrated the extremely fast response time which facilitates detecting reactive

species produced in the flame front and the extremely fast cooling rate which "freezes" the chemical reaction and facilitates measuring the composition.

Under Air Force Contract FO 4611-69-c-0083, Kahrs [11] at Thiokol Chemical Corporation designed a molecular-beam gas sampling apparatus for high-pressure high-temperature rocket-motor applications. Only modest success was realized. A serious problem was the heat transfer to the water-cooled skimmer. The exhaust gas of the rocket motor was evacuated entirely by the source-chamber pumping system. A relatively small value of stagnation-chamber pressure/source-chamber pressure resulted. Hence the skimmer had to be located relatively close to the sampling source in order to avoid Mach-disk interference. The resulting high heat-transfer rate produced a water leak near the water-cooled tip of the skimmer after only two tests. This sampling system was subsequently transferred from Edwards Air Force Base to JPL for possible use.

The system described in this report is modified (almost completely) from the system designed by Kahrs. Major changes include the use of a water-cooled end plate and a heat-shield assembly so that most of the rocket plume gas is exhausted into the atmosphere thereby reducing the pumping load. Consequently, the heat-transfer rate to the skimmer tip is negligible so that no cooling is required. A complete new detection chamber facilitates housing the mass-spectrometer detector in either the cross-beam or the axial-beam position.

II. DESIGN PARAMETERS

In this chapter, problems associated with rocket samplings are described. Several useful design equations are given.

A. Problems Associated with Rocket Samplings.

In the design of a rocket sampling system, one has to consider the following problems: (1) the nonuniformity of the flow inside the combustion chamber, (2) the high temperature and high pressure inside the combustion chamber, and (3) the highly corrosive nature of the propellants. The first problem requires that the sampling system does not disturb the nonuniform properties of the flow. The second problem requires high pumping speed. (Note that a lower limit for the sampling-orifice diameter is imposed by the needs to provide adequate cooling to the sampling orifice and to reduce boundary-layer effects. A large mass flow rate results then since the mass flow rate is proportional directly to the square of the orifice diameter, directly to the chamber pressure, and inversely to the square root of the chamber temperature.)

B. Equation for Gases Flowing Through a Sonic Nozzle.

If the flow through the nozzle is sonic, then the flow rate equals the product of the sonic speed, the gas density, and the nozzle area, all evaluated (for convenience) at the throat. For a thermally perfect gas, one can show that

$$\dot{M} = \frac{\pi}{4}\sqrt{\frac{m\gamma}{kT_o}}\left(\frac{\gamma+1}{2}\right)^{-\frac{\gamma+1}{2(\gamma-1)}} p_o d^{*2} \qquad (1)$$

where $\dot{M}$ is the mass flow rate, T_o is the stagnation temperature, d^* is the effective nozzle diameter, p_o is the stagnation pressure, m is the (mean) molecular weight of the gas (mixture), k is the Boltzmann constant,

and γ is the (mean) specific heat ratio of the gas. It is seen that, although the high temperature T_o encountered in rocket sampling reduces the required mass pumping rate, it is dominated by the high chamber pressure p_o.

C. Equation for Gases Flowing Through a Pumping System.

The thermodynamic equation of state of the gas inside the vacuum chamber can be written

$$pV = M(R_u/m)T \tag{2}$$

where p, V, T are respectively the vacuum chamber pressure, volume, and temperature, R_u is the universal gas constant, M is the total mass of the gas inside the vacuum chamber, and m is the (mean) molecular weight of the gas. Hence, for a vacuum chamber operating at constant pressure and temperature, the volume pumping rate $\dot{V}$ is related to the mass pumping rate by

$$p\dot{V} = \dot{M}(R_u/m)T \tag{2}'$$

D. The Free-Jet Parameters.

When a gas expands from a high-pressure source into a partially evacuated chamber, a shock structure such as shown in Fig. 3 is observed. Parameters important in a molecular-beam system design include the Mach disk location x_M and the centerline Mach number M_i. The former can be predicted quite accurately using [12]

$$x_M/d^* = 0.67(p_o/p_s)^{\frac{1}{2}} \tag{3}$$

where p_o and p_s are respectively the stagnation-chamber pressure and the source-chamber background pressure. In a molecular beam system, since almost all of the gases flowing through the sampling nozzle are

evacuated by the source-chamber pumping system, one can combine Eqs. (1), (2)', and (3) to obtain

$$x_M/d^* = 0.67 \sqrt{\frac{4}{\pi}} \sqrt[4]{\frac{kT_o}{m\gamma}} \left(\frac{\gamma+1}{2}\right)^{\frac{\gamma+1}{4(\gamma-1)}} \frac{\sqrt{\dot{V}_s}}{d^*} \sqrt{\frac{m}{R_u T}} \tag{4}$$

or

$$x_M = 0.67 \sqrt{\frac{4}{\pi}} \sqrt[4]{\frac{mkT_o}{\gamma}} \left(\frac{\gamma+1}{2}\right)^{\frac{\gamma+1}{4(\gamma-1)}} \sqrt{\frac{1}{R_u T}} \sqrt{\dot{V}_s} \tag{4}'$$

Supersonic molecular-beam sampling is possibly only when the skimmer tip is located upstream from the Mach-disk location. The optimum location depends on the stagnation pressure, source-chamber pressure, and skimmer geometry [13]. The Mach disk location depends on the pumping speed V_s, but not the nozzle diameter or the pressure level. (For a constant V_s, a change in p_o results in a change in p_s, but the ratio of the two pressures remains constant.) This observation is particularly important in designing a source-chamber pumping system for high-pressure sampling. Since most conventional supersonic molecular beam systems use high-throughput oil booster pumps for evacuating the source chamber, the speed of the pumping system drops considerably if the source chamber pressure exceeds 10^{-1} torr, and a small value of x_M results. Mechanical pumps, on the other hand, operate at relatively high source-chamber pressure without losing pumping speed. Therefore, a high-pressure high-throughput system which would require an excessively costly booster pump can be handled by a mechanical pump of reasonable size.

Values of the centerline Mach number are needed for estimating the mass-flow rate through the skimmer. In ref. 12, the following numerical expressions for the centerline Mach number M_i at distance x downstream

from the orifice are obtained:

$$M_i = 3.26\left(\frac{x}{d^*} - 0.075\right)^{0.67} - \frac{0.536}{(x/d^* - 0.075)^{0.67}} \quad \text{for } \gamma = 5/3 \qquad (5)$$

$$= 3.65\left(\frac{x}{d^*} - 0.40\right)^{0.4} - \frac{0.822}{(x/d^* - 0.40)^{0.4}} \qquad = 7/5 \qquad (5)'$$

$$= 3.96\left(\frac{x}{d^*} - 0.85\right)^{0.286} - \frac{1.01}{(x/d^* - 0.85)^{0.286}} \qquad = 9/7 \qquad (5)''$$

E. Pumping Load Required for a Collimating Chamber.

The mass flow rate through the skimmer is

$$\dot{M}_1 = \rho_1 A_1 u_1$$

$$= \rho^* A^* u^* \frac{A_1}{A^*} \frac{\rho_1}{\rho^*} \frac{u_1}{u^*}$$

$$= \dot{M}\left(\frac{d_1}{d^*}\right)^2 \frac{\rho_1}{\rho^*} \frac{M_1 a_1}{M^* a^*}$$

$$= \dot{M}\left(\frac{d_1}{d^*}\right)^2 \frac{\rho_1}{\rho^*} M_1 \left(\frac{T_1}{T^*}\right)^{1/2} \qquad (6)$$

where ρ is density, subscript 1 designates the skimmer and superscript * represents the sonic throat. Then, using the following continuum isentropic relationships

$$\frac{\rho_1}{\rho^*} = \left(\frac{1 + \frac{\gamma-1}{2} M^2}{\frac{\gamma+1}{2}}\right)^{-\frac{1}{\gamma-1}}$$

and

$$\frac{T_1}{T^*} = \left(\frac{1 + \frac{\gamma-1}{2} M^2}{\frac{\gamma+1}{2}}\right)^{-1}$$

one obtains

$$\dot{M}_1 = \dot{M}\left(\frac{d_1}{d^*}\right)^2 M_1 \left[\frac{2}{\gamma+1}\left(1 + \frac{\gamma-1}{2} M_1^2\right)\right]^{-\frac{\gamma+1}{2(\gamma-1)}} \tag{7}$$

The flow through the skimmer is essentially the sole pumping load for the collimating chamber. Then, using Eq. (2), one obtains

$$p_c \dot{V}_c = \dot{M}_1 (R_u/m) T_c \tag{8}$$

where T_c is the collimating-chamber (room) temperature. Combining Eqs. (7), (8) and (1), one obtains

$$\dot{V}_c = \frac{\pi}{4}\sqrt{\frac{m\gamma}{kT_o}}\left(\frac{\gamma+1}{2}\right)^{-\frac{\gamma+1}{2(\gamma-1)}} M_i \left[\frac{2}{\gamma+1}\left(1 + \frac{\gamma-1}{2} M_i\right)\right]^{-\frac{\gamma+1}{2(\gamma-1)}} d_1^2 \frac{p_o}{p_c} \tag{9}$$

It is seen that the required collimating-chamber pumping speed is directly proportional to the combustion-chamber pressure p_o and inversely proportional to the collimating-chamber pressure p_c. The higher the value of p_c, the greater the beam attenuation due to background scattering inside the collimating chamber. However, if the product of p_c and L_{12} (i.e., the attenuation distance between the skimmer and collimating orifices) is less than 10^{-3} torr-cm, then the mean-free-path length for beam-background collisions is approximately five times greater than the scattering length, and background scattering can be neglected. It is therefore advantageous to design a system with short L_{12} (without choking the flow in the postskimmer region) so that reasonable sampling can be obtained under the relatively high collimating-chamber pressure p_c encountered in a high-pressure sampling system can be tolerated.

F. Summary

In summary, one obtains the following working formulas for a rocket system using N_2H_4/N_2O_4 as the propellants. (Assuming T_o = 4500°R, m = 20, and γ = 9/7):

The Mass Flux through the sampling orifice:

$$\dot{M} = 0.074\ p_o d^{*2}$$

with

$\dot{M}$ in lb/sec

p_o in ATM

d^* in inch

The Mach-Disk Location:

$$x_M = 0.072(\dot{V}_s)^{\frac{1}{2}}$$

with

x_M in in. and $\dot{V}_s$ in CFM

The Centerline Mach Number (ideal):

$$M_i = 3.96(x_1/d^* - 0.85)^{0.286} - 1.01/(x_1/d^* - 0.85)^{0.286}$$

where

x_1 is the nozzle skimmer distance

The Collimating Chamber Pumping Requirement:

$$p_c\dot{V}_c = 31100\ d_1^2\ p_o M_i [0.875(1 + 0.14285\ M_i^2)]^{-4}$$

where

$\dot{V}_c$ is in liter/sec and p_c is in torr.

Figure 4 shows the alignment chart relating the combustion-chamber pressure p_o, the source-chamber pressure p_s, the sampling-orifice diameter d^*, and the Mach number M_i at the skimmer tip. Figure 5 shows the alignment chart for obtaining the throughput of the collimating chamber, $p_c\dot{V}_c$, for various p_o and x_1.

III. SYSTEM DESCRIPTION

In this chapter, descriptions are given for the various vacuum chambers, the beam-formation components, and the interface between the rocket and the molecular-beam system. Most of the system components, except the collimation chamber (which was modified from the Thiokol system), were designed and built during this funding period. All parts drawing numbers are listed in the Assembly Drawing JPL No. 10038852. Figure 7 is a photograph of the completed rocket-chamber sampling system.

A. The Vacuum System

The vacuum system consists of three stages; the source chamber, the collimating chamber, and the detection chamber. The source chamber is pumped solely by a 300 CFM Stokes mechanical pump. For a sampling nozzle of 0.031-in. diameter, the estimated source-chamber pressure p_s ranges from 0.2 to 4.4 torrs (see Fig. 4) for combustion-chamber pressures from 1 atm to 20 atm. The collimating chamber is pumped by a 6-in. diffusion pump backed by a Kinney mechanical pump. For the above mentioned sampling nozzle size and combustion-chamber pressure range, the estimated collimating chamber pumping load ranges from 0.006 to 0.12 torr-liter/sec. Since the 6-in. oil diffusion pump has a pumping capacity of the order of 1500 liters/sec, the estimated collimation-chamber pressure p_c, for a nozzle-skimmer distance of $x_1 = 0.75$ in., ranges from 4×10^{-6} to 8×10^{-5} torr. The detection chamber is pumped by a 4-in. oil diffusion pump backed by a Welch mechanical pump. The operating detection-chamber pressure is of the order of 10^{-6} torr.

B. The End Plate (JPL Drawing No. 10038840)

The Laval nozzle of an ordinary rocket engine has been replaced by a stainless-steel water-cooled end plate with 29 holes (dia = 0.147 in.) to

facilitate sampling from different locations (see Fig. 7). The holes are uniformly distributed in order to preserve the (nonequilibrium) thermodynamic state of the combustion gases (particularly the nonuniform fuel/oxidizer distribution).

C. The Rocket Engine Mounting Plate (JPL Drawing No. 10038841)

A stainless-steel plate facilitates mounting the rocket chamber together with the end plate. This plate assembly is then mounted on the molecular beam heat-shield unit via six slotted holes. The rocket chamber can be rotated angularly and moved radially with respect to the molecular-beam system.

D. The Heat-Shield Assembly (JPL Drawing No. 10038839)

The stainless steel heat-shield unit as shown in Fig. 8 is constructed as part of the source chamber. On the outer surface facing the end plate are 113 0.04-in.-dia. holes which inject water radially. This water injection (a) prevents the hot gas from overheating the vacuum system, and (b) water-scrubs the dissolvable gases, particularly the harmful unburned fuel and oxidizer. The internal angle of the cone-shaped heat shield unit is 100°. A 0.031-in. dia. sampling orifice is located at the tip of the heat shield. Further details of the sampling orifice are given in JPL Drawing No. 10038838.

E. The Skimmer Assembly

The skimmer assembly consists of two parts: the skimmer tip, made of copper (JPL Drawing No. 10038842); and the skimmer base, made of stainless steel (JPL Drawing No. 10038848). The former is threaded into the latter. The external and internal half angles of the skimmer tip are

30° and 15° respectively; the tip diameter is 0.02 in. The half angle and length of the skimmer base are 25° and 4.30 in. respectively. Several stainless steel spacers with different thicknesses are used to vary the nozzle-skimmer distance from 0.21 to 1.50 in. The data reported in the next chapter were taken at a nozzle-skimmer distance of 0.75 in., corresponding to $x_1/d^* \approx 24$.

F. The Beam Detector

The beam detector employed here is the EAI 200 Quadrupole mass spectrometer. The present configuration of the ionizer permits it to be used only in the cross-beam position. However, the detection chamber is designed so that the detector can be used in both the cross-beam and axial-beam positions.

IV. EXPERIMENTAL RESULTS

The sampling system has been operated in tests of (a) cooling-water flow rates, (b) spacing between the end plate and the sampling nozzle, and (c) sampling capability.

A. Cooling-Water Flow Rate

Cooling-water flow rates were measured for the rocket end plate and the heat-shield unit. For inlet pressure of 60 psig and outlet pressure of 1 atm, the respective water flow rates are approximately 6 and 22 GPM. The end plate cooling-water temperature rose, during the rocket firing tests, only approximately 20°C for a combustion-chamber pressure of 200 psig. The temperature rise of the heat-shield-unit cooling water was not measured.

B. Spacing Between the End Plate and the Sampling Nozzle

In order to obtain an appropriate gas flow rate through the sampling region, the spacing between the end plate and the heat shield is made adjustable. If the gap is too large, then the flow inside the gap region becomes supersonic; a normal shock would then form prior to the sampling orifice and the shock heating might distort the chemical concentrations. Otherwise, if the gap is too small, then the flow becomes partially stagnant which also might distort the chemical concentrations. Results of a series of cold flow simulations are shown in Fig. 9. It is seen that the optimum spacing is approximately one-fourth of the nozzle diameter.

C. Sampling Capability

A series of rocket firing tests has been performed using the highly reactive propellants nitrogen tetroxide/hydrazine (N_2O_4/N_2H_4) at an

oxidizer/fuel ratio of 1.23 by weight. Figure 10 shows the sampling positions located on the injector plane. The duration of each rocket firing test was 6 seconds (limited by the non-cooled rocket chamber). The combustion-chamber pressure was 60 psig. The nozzle-skimmer distance x_1/d^* was 24. Relevant experimental parameters, including the fuel and oxidizer tank pressures, the combustion-chamber pressure, the fuel and oxidizer valve actuations, and the mass spectrometer output signals (in logarithmic scale), were automatically monitored from 5 seconds before ignition to 5 seconds after ignition by a multi-channel graphic recorder.

Figure 11 shows the time histories of the combustion chamber pressure and several mass-spectrometer signals for data taken at the extreme oxidizer-side sampling position. Time is measured from the instant when the oxidizer (N_2O_4) solenoid valve is triggered. (The fuel solenoid valve is triggered 0.06 second thereafter.) It is seen that the pressure began to rise at $t \simeq 0.7$ sec and reached steady state at $t \simeq 1.8$ sec. The first 0.7 sec might correspond to the time required to transport the propellants from the solenoid valves to the impingement plane. The subsequent 1.1 sec might be the combustion-chamber charging time. No popping was observed (neither during the test nor in Fig. 12) under the testing conditions. The pressure increase after the closure of the solenoid valves was due to the high-pressure nitrogen purge of the propellant lines which produced abnormally high propellant flows. The mass spectrometer scanned, to m/e = 48, at a rate of 1.7 sec/sweep. Consequently the data for different masses were taken at different times. The signals are expressed in logarithmic scale; each decade is marked automatically from the calibration circuit. Note that the traces prior to the firing were steady, indicating a stable background (and room-temperature beam). The traces were quite

steady also during the steady combustion period. The signals during the transient ignition and shutdown periods are not reliable and therefore are indicated by broken lines. Since the samples were taken at the extreme of the oxidizer side, a relatively high concentration of unburned fuel is expected prior to the complete development of the spray fan (i.e., the fuel would penetrate toward the oxidizer side). This explains the peaking of the m/e = 1 trace at t ≃ 0.8 sec. Similar reasoning explains also the m/e = 31 trace (i.e., N_2H_3, a fragment from N_2H_4). If one compares the m/e = 17 and 18 traces, one finds that the m/e = 17 intensity exceeds the fragment contribution from water (judged from prefiring traces), particularly during the transient period, due primarily to the presence of NH_3 in the beam. No peaking is expected for the oxidizer traces during the transient stage. (The profiles of m/e = 46, the NO_2 peak, and of m/e = 30, contributed mostly from NO, support this statement.) The m/e = 32, 28, 16 and 14 backgrounds were indeterminable due to the presence of a beam of purging nitrogen and residual air prior to firing. Therefore, the contributions to these traces from combustion gases also are indeterminable and are not shown in Fig. 11. A beam flag has been installed recently to facilitate subtracting the room-temperature beam signals from the background signals.

The signals after shutdown are higher than the pre-firing signals. Two possible explanations are being considered: (a) Shortly after the shutdown, the sampling orifice still samples gases left inside the combustion chamber. (This explanation is supported by observations that the post-run nitrogen signals were lower than the pre-run values.) (b) The post-run pressures (and hence the background signals) inside the collimation and detection chambers are increased.

In Fig. 12(a)-(g) the mass spectra are given for seven different sampling locations. The open symbols represent signals prior to ignition while the filled points indicate signals observed during the combustion. Note that the mass range covers up to m/e = 32 only. Also note that only those peaks which showed significant changes during combustion are shown. Background intensities change some from run to run, due mainly to the fact that these data were taken over two days (drift in vacuum-chamber pressures cannot be avoided). All these seven runs show unburned fuel since the mixture ratio of 1.23 is a stoichiometrically fuel-rich mixture. Among these seven runs, the one obtained at location F2 (2 holes from the center toward the fuel side) shows the most complete combustion. Note that the data presented here have not been adjusted for mass-spectrometer sensitivities; therefore, quantitative interpretations are not possible at this time.

V. DISCUSSIONS AND CONCLUSIONS

A molecular-beam mass-spectrometer system has been successfully developed and tested for direct sampling from a hypergolic-liquid-propellants rocket-motor combustion chamber. Unique design features of the sampling system include (a) the use of a multi-nozzle end-plate for preservation of the non-uniform properties of the flow field inside the combustion chamber, (b) the use of a water-injection heat shield, and (c) the use of a 300 cmf mechanical pump for the first vacuum stage (eliminating the use of a huge conventional booster pump).

Several convenient design equations are presented. The most useful equation is perhaps Eq. (4)' which determines the location of the Mach disk. To obtain a supersonic beam, the skimmer must be located upstream from the Mach disk (a necessary but not sufficient condition). It has been shown that the Mach-disk location depends on, among other things, the pumping speed of the first chamber $\dot{V}_s$, but not (directly) on the sampling source pressure p_o; generation of a supersonic molecular beam is possible as long as the pumping speed is large enough to sustain a sufficient pressure ratio p_o/p_s.

In a high-pressure sampling system, the skimmer tip is located in a relatively high density region (compared with a low-pressure sampling system). The beam is thus more prone to skimmer interference. Therefore, skimmer cone angle and skimmer diameter are critical design parameters. The cone angle of the skimmer designed here is such that an attached shock is realized. The skimmer-orifice diameter of 0.02 in. was chosen for fabrication convenience. In future work, it is desirable to fabricate a skimmer tip with different diameter for comparisons. The sampling data

reported here were obtained using a nozzle-skimmer distance of $x_s/d^* = 24$. More tests are needed to optimize the skimmer position.

It has been occasionally observed that, prior to rocket ignition, the cooling water ejected from the heat-shield unit penetrated the sampling nozzle. Then all the vacuum-chamber pressures increase considerably (and erratically) due to the evaporation of the water droplets. Under such circumstances, it is necessary to turn off the mass spectrometer immediately in order to prevent destructive arcing due to high gas density inside the detection chamber. This difficulty has been reduced considerably by increasing the purging-nitrogen flow rate.

The mass spectrometer ionizer is currently installed as a cross-beam detector. A slight modification in the ionizer is needed for the axial-beam position. It is expected that the axial-beam mode of operation will yield a greater beam-to-background signal ratio. This advantage should be explored.

The use of the logarithmic amplifier in the mass-spectrometer data processings enhances the detection of weak signals. However, its slow response time limits the sweep rate of the mass spectrometer. A fast sweep rate is essential for temporal studies of the unstable combustion anticipated in future work. Therefore, improvement in the Log-Amplifier is strongly suggested.

The experiments performed to date provide only a preliminary evaluation of the beam performance. The presented mass-spectrometer data have not been adjusted for fragmentations by the ionizer, sensitivity of the mass spectrometer, and compositions distortions during the sampling process [14]. Therefore, no quantitative conclusions should be drawn from these preliminary data.

In spite of the uncertainties mentioned above, the sampling data indicate the coexistance of fuel and oxidizer species in the beam, an important observation which was not expected in a hypergolic propellant system.

ACKNOWLEDGMENTS

The design, fabrication, assembly, and testing of the apparatus were made possible by the contributions of Mr. Wayne Rodgers of UCLA, and Messrs. Fred Gerbracht, Jay Garcia and Jim Kizziar of JPL. Their assistance is deeply appreciated.

REFERENCES

1. Elverum, G. W., Jr., and Staudhammer, P., Progress Report 30-4, Jet Propulsion Laboratory, Pasadena, Calif., Aug. 25, 1959.

2. Kushida, R., and Houseman, J., Technical Memorandum 33-395. Jet Propulsion Laboratory, Pasadena, Calif., July 1968. Also paper WSCI-67-38, Western States Combustion Institute, Seattle, Wash., 1967.

3. Houseman, J., AIAA J. 8:597-599, March 1970.

4. Foner, S. N., Advances in Atomic and Molecular Physics, (D. R. Bates and I. Estermann, eds.), Vol. 2, pp. 385-461, Academic Press, New York, 1966.

5. Greene, F. T., and Milne, T. A., AIAA Paper 67-37, presented at AIAA 5th Aerospace Sciences Meeting, New York, January 23-26, 1967.

6. Sturtevant, B., and Wang, C. P., Recent Advances in Aerothermochemistry (I. Grassman, ed.), Vol. 2, NATO Advisory Group for Aerospace Research and Development, Paris, 1967, pp. 595-606.

7. Dix, R. E., AEDC-TR-69-37, ARO Inc., Arnold Air Force Station, Tennessee, April 1969.

8. Chang, J. H., AIAA Paper 69-64, presented at the AIAA 7th Aerospace Sciences Meeting, New York, January 20-22, 1969.

9. Knuth, E. L., to be published in Engine Emissions (G. S. Springer and D. Patterson, eds.). Plenum Publishing Co., 1973.

10. Young, W. S., Wang, Y. G., Rodgers, W. E., and Knuth, E. L., Technology Utilization Ideas for the 70's and Beyond, American Astronautical Society, Tarzana, 1971, pp. 281-289.

11. Kahrs, J., AFRPL-TR-70-28, Air Force Rocket Propulsion Laboratory, California, Edwards, March 1970.

12. Ashkenus, H., and Sherman, F. S., Rarefied Gas Dynamics (J. H. deLeeuw, ed.), Vol. II, pp. 84-105. Academic Press, New York, 1966.

13. Bossel, U., Hurlbut, F. C., and Sherman, F. S., Rarefied Gas Dynamics (L. Trilling and H. Y. Wachman, eds.), Vol. II, pp. 945-964. Academic Press, New York, 1969.

14. Knuth, E. L., and Young, W. S., presented at the Molecular Beam Sampling Conference, Lake of the Ozarks, Missouri, Oct. 25-27, 1972.

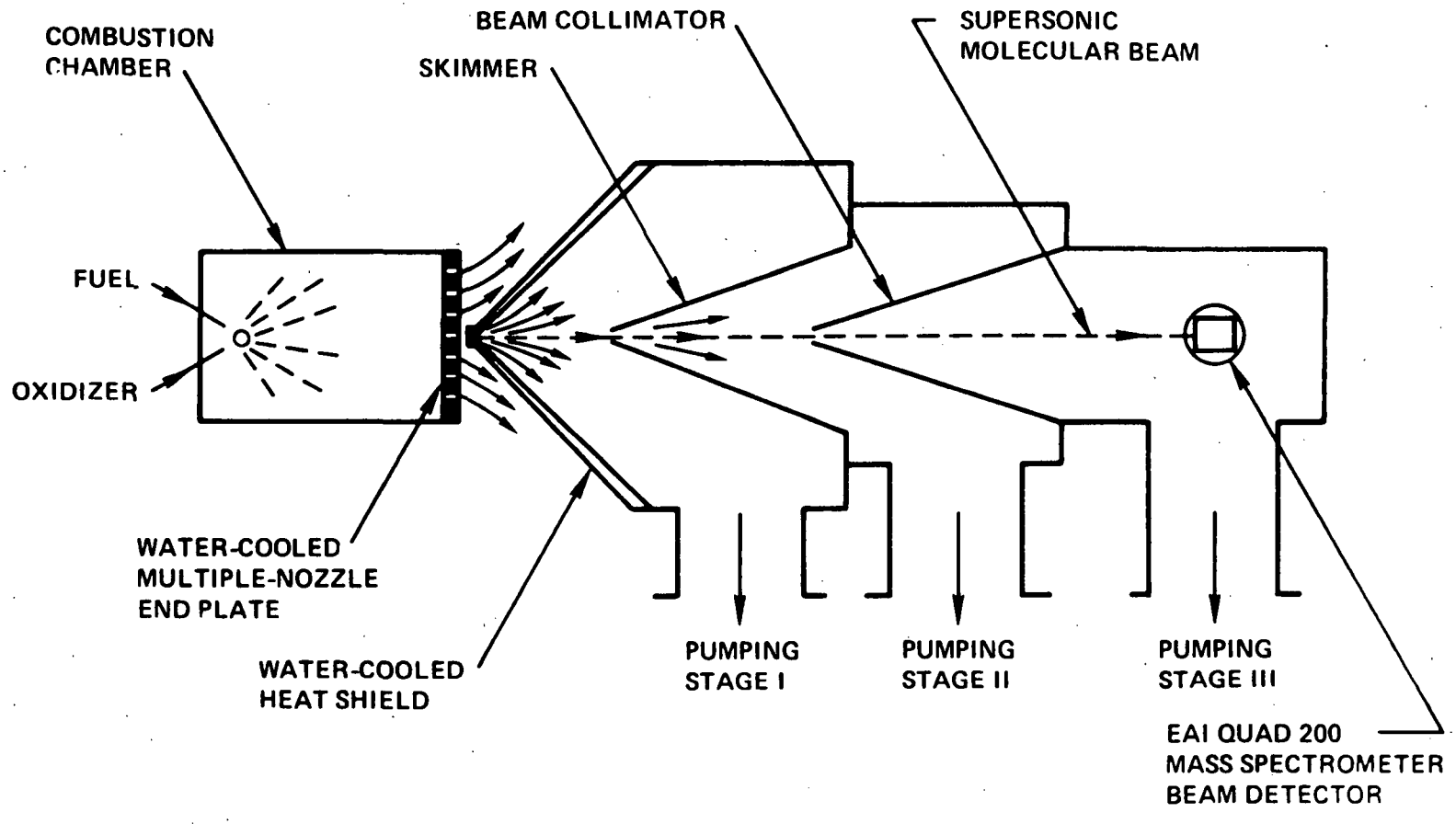

Figure 1. Molecular-Beam Sampling System Applied to Rocket-Motor Studies.

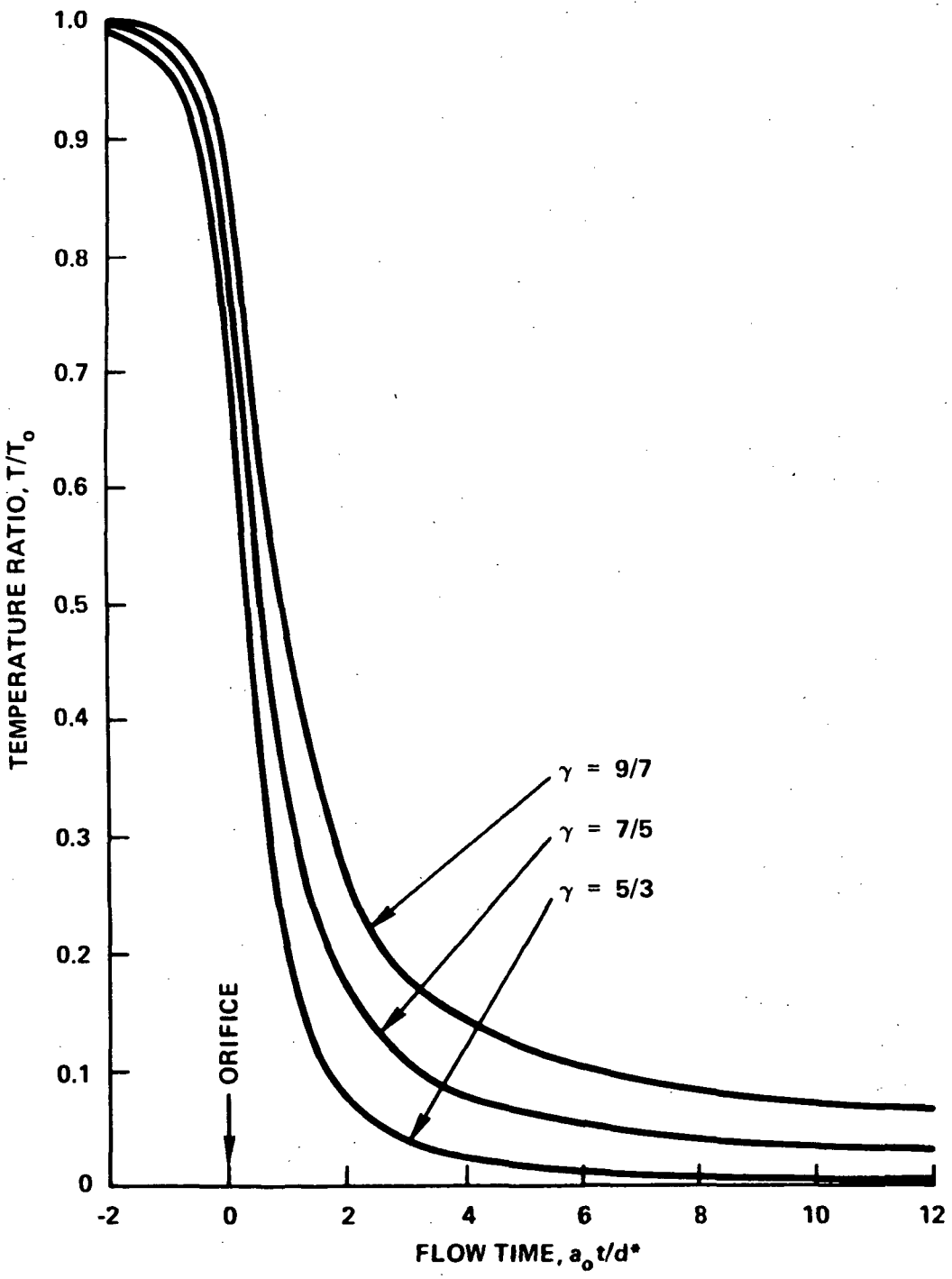

Figure 2. Temperature Ratio as Function of Dimensionless Flow Time for Free-Jet Gas Flows from Orifice.

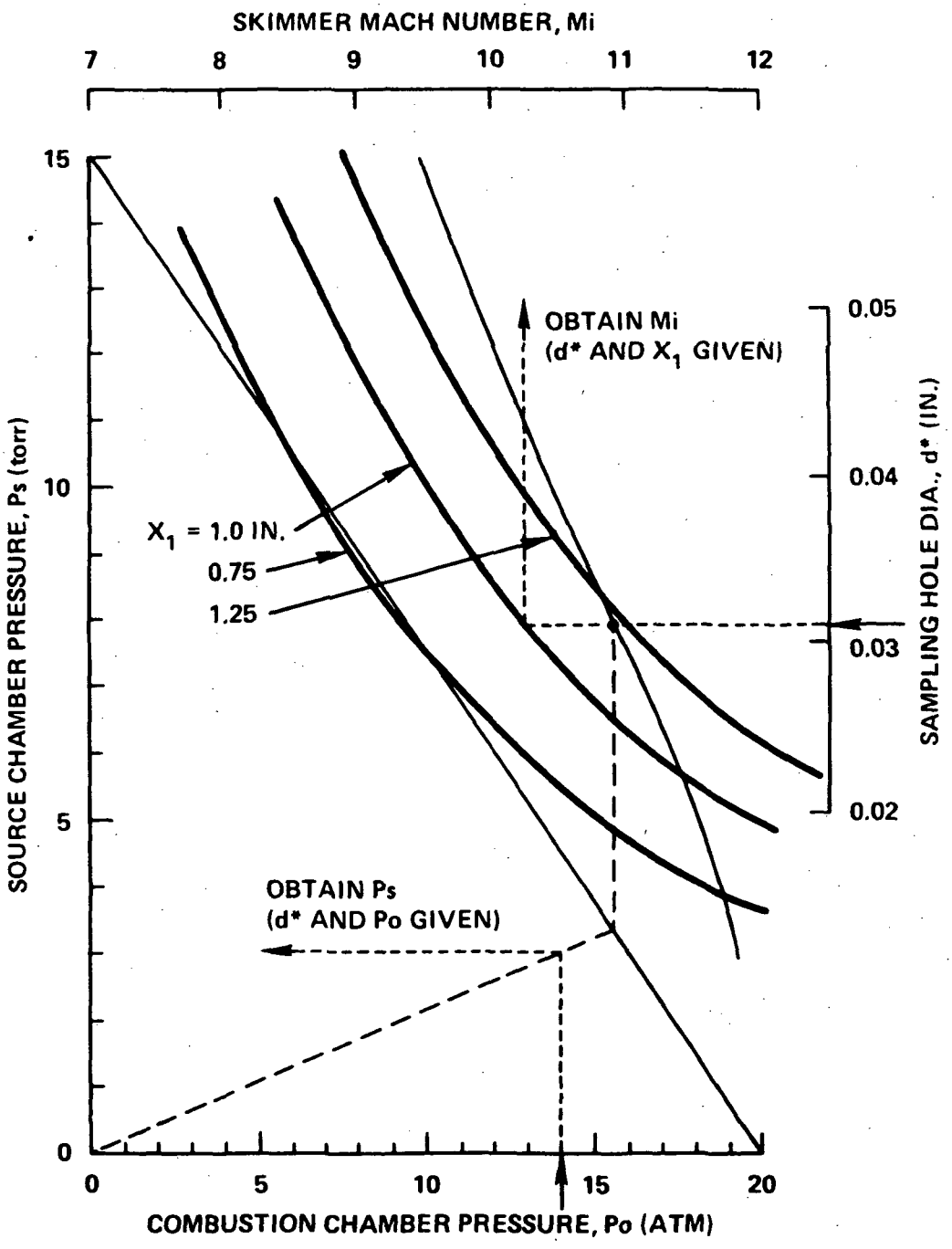

Figure 4. Source Chamber Pressure P1 and Skimmer Mach Number Mi as Functions of Combustion Chamber Pressure Po and Sampling Hole Dia. d*. Source Chamber Pumping Speed $\dot{V}s$ = 300 CFM.

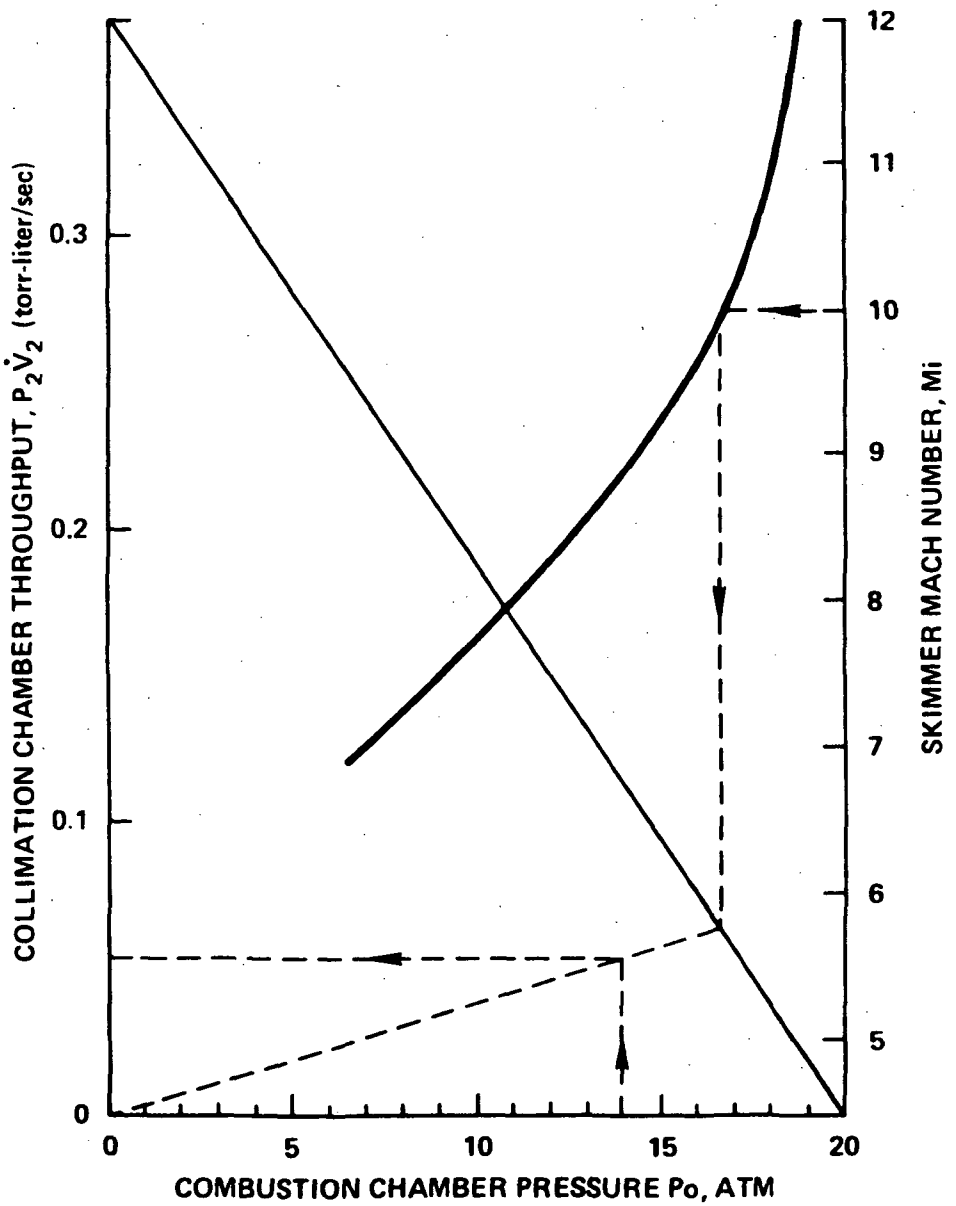

Figure 5. Collimating Chamber Throughput $P_c\dot{V}_c$ as a Function of Combustion Chamber Pressure Po and Skimmer Mach Number. Skimmer Dia. d_1 = 0.02 In.

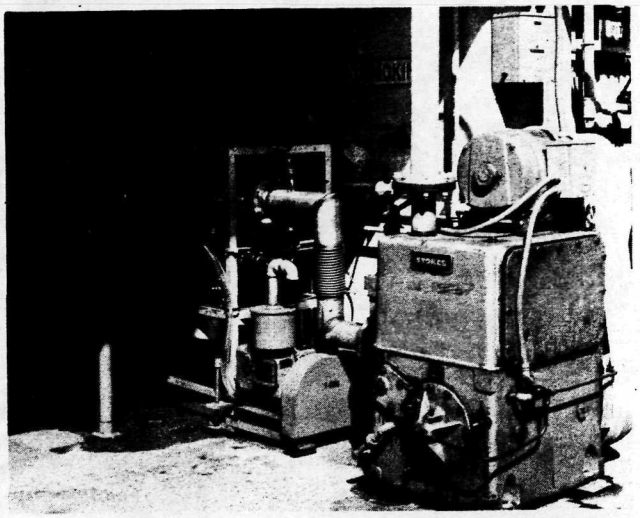

Figure 6. The Completed Rocket-Chamber Sampling System.

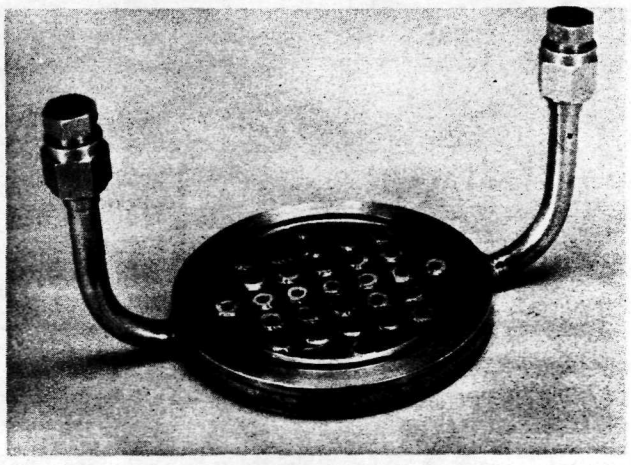

Figure 7. The Water-Cooled Multiple-Nozzle End Plate.

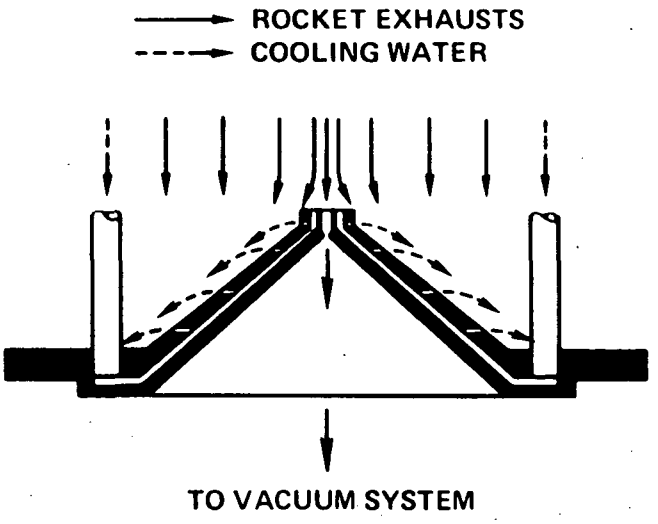

Figure 8. The Water-Cooled Heat Shield

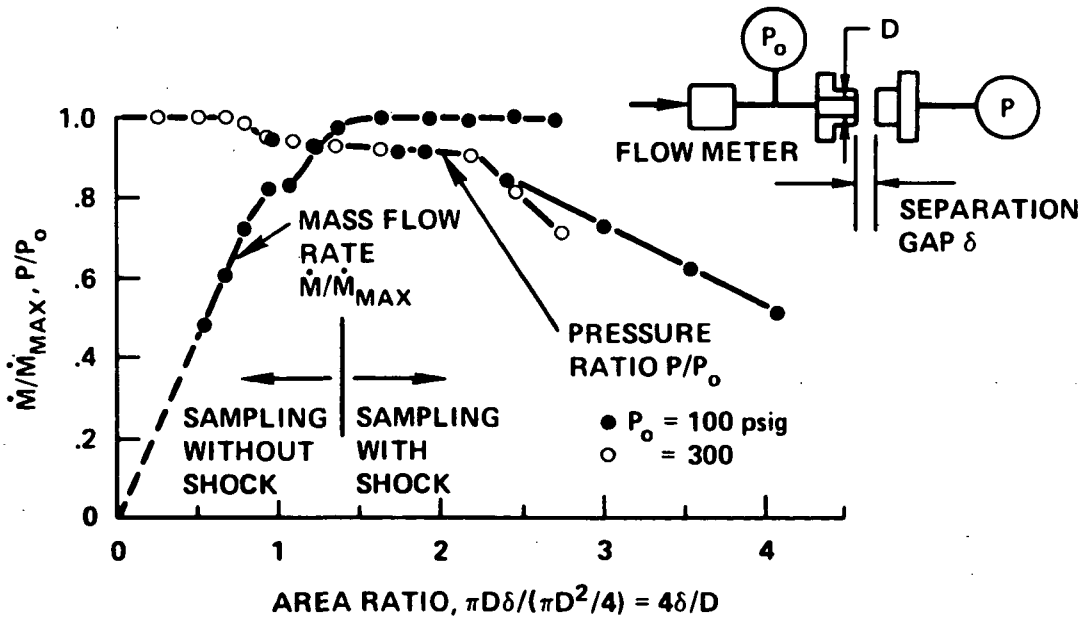

Figure 9. The Flow Rate and Pressure Ratios versus the Separation Gap.

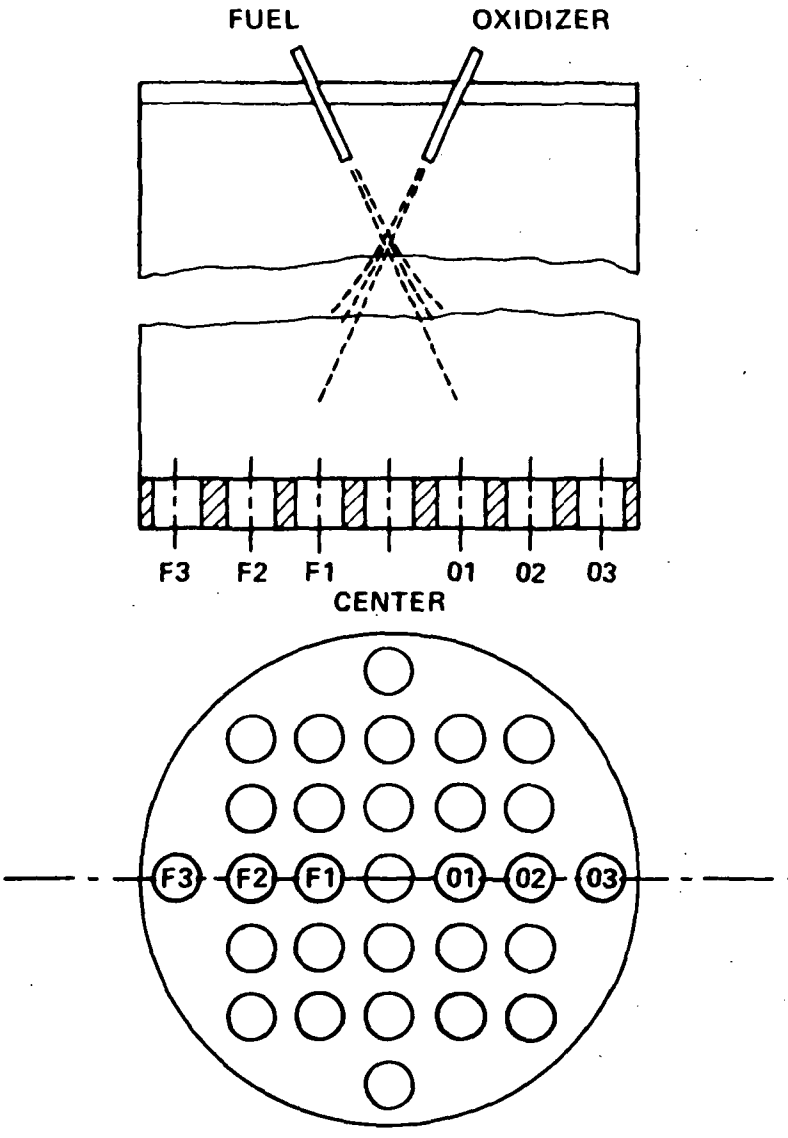

Figure 10. Sampling Location on Injector Plane.

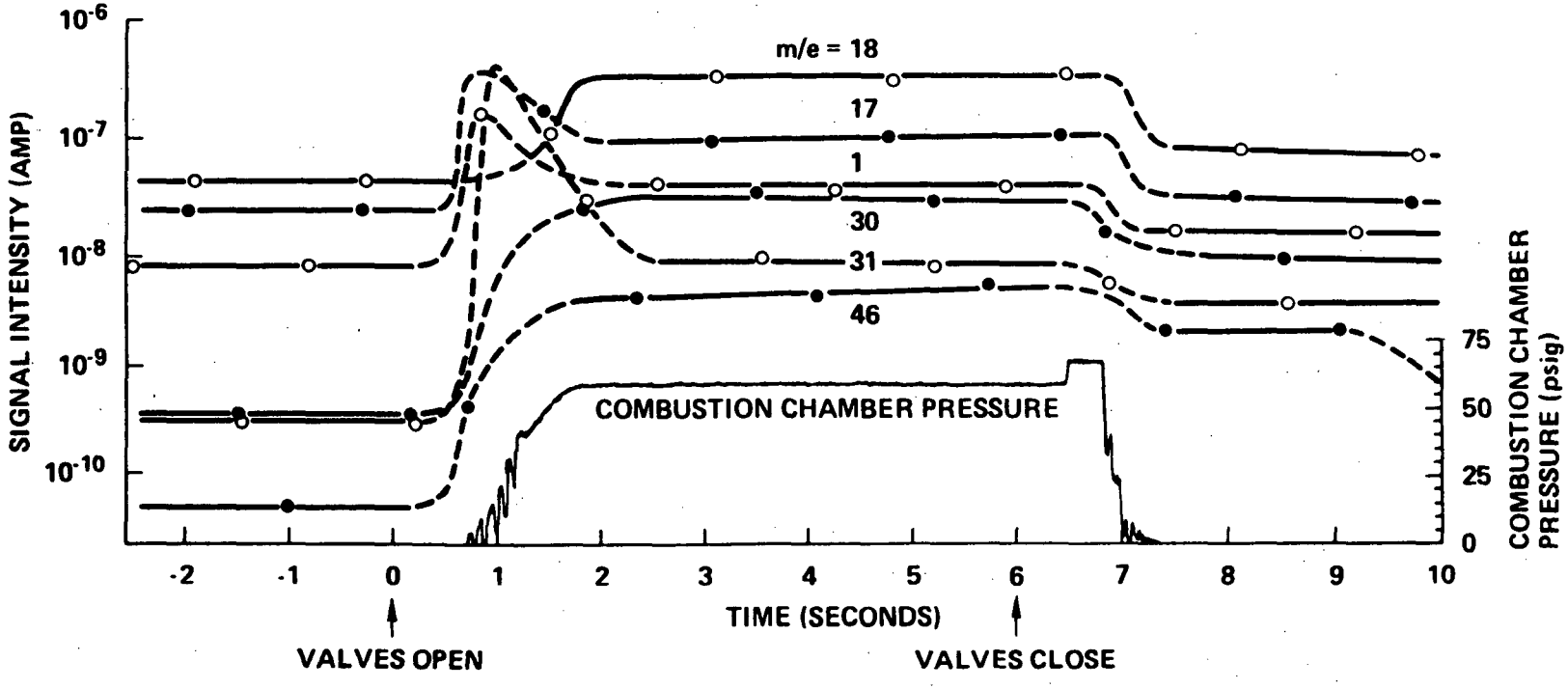

Figure 11. Temporal Profiles of the Combustion Chamber Pressure, Po, and the Mass-Spectrometer Traces.

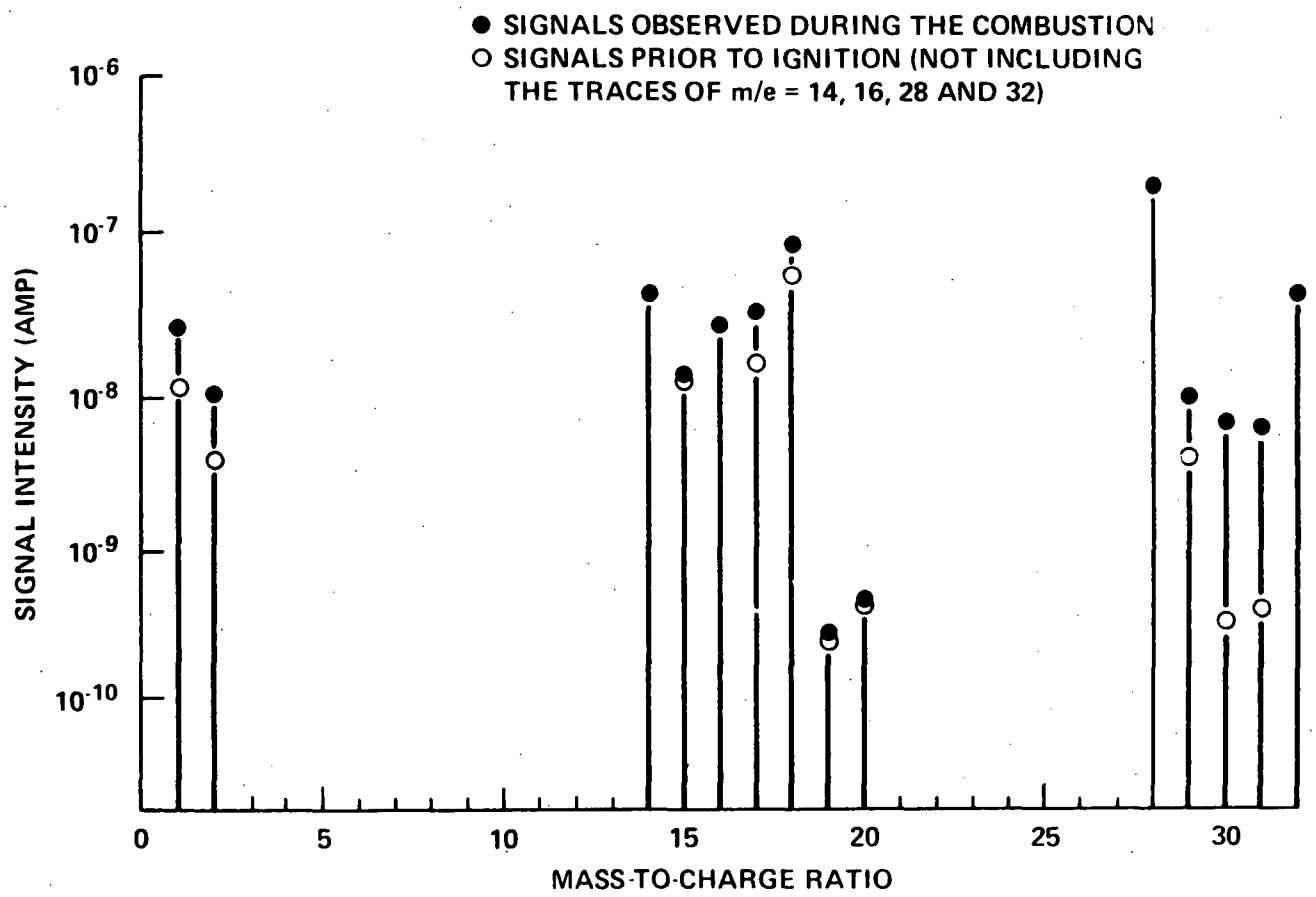

Figure 12(a). Mass Spectrum Observed at Sampling Location F3.

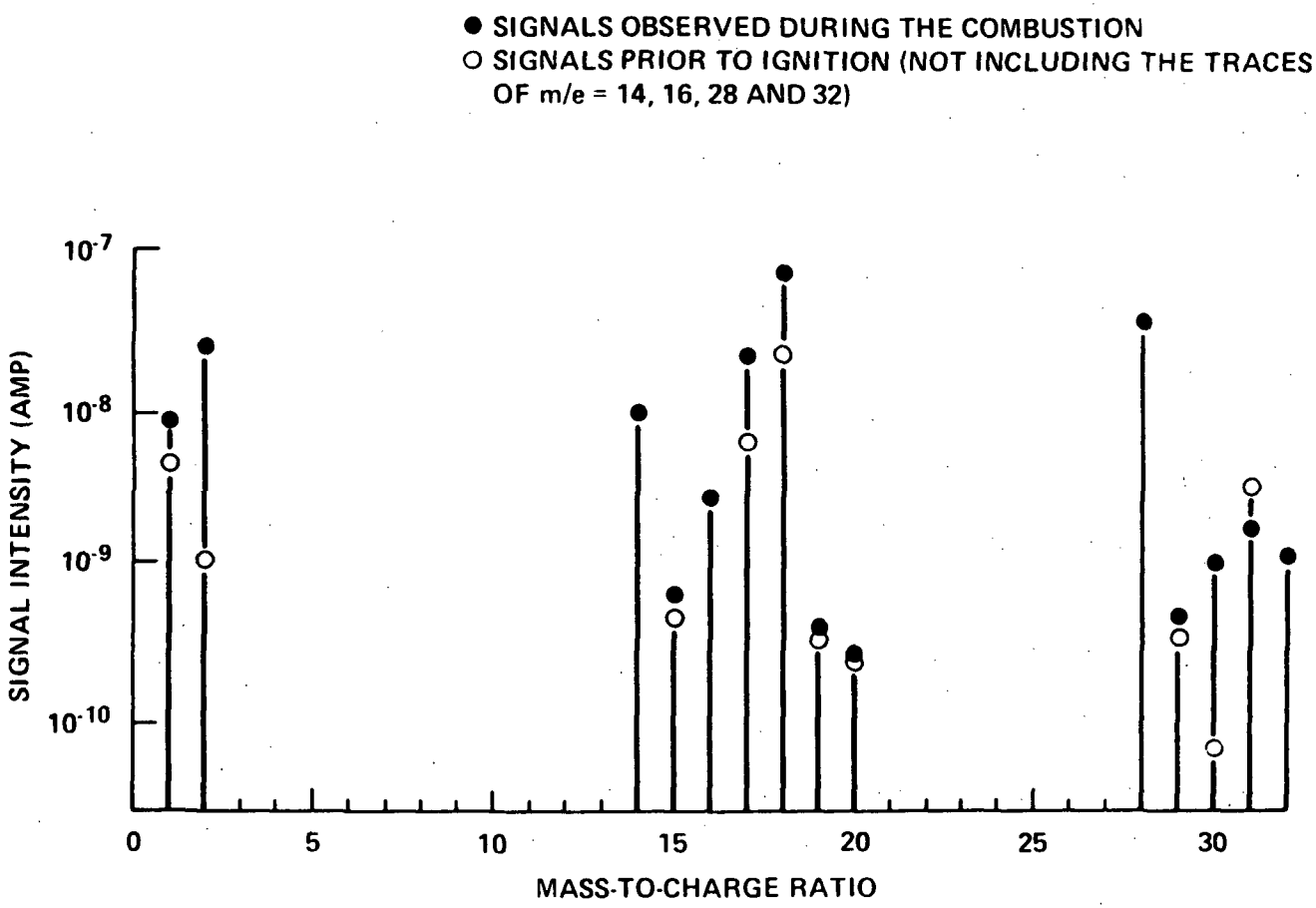

Figure 12(b). Mass Spectrum Observed at Sampling Location F2.

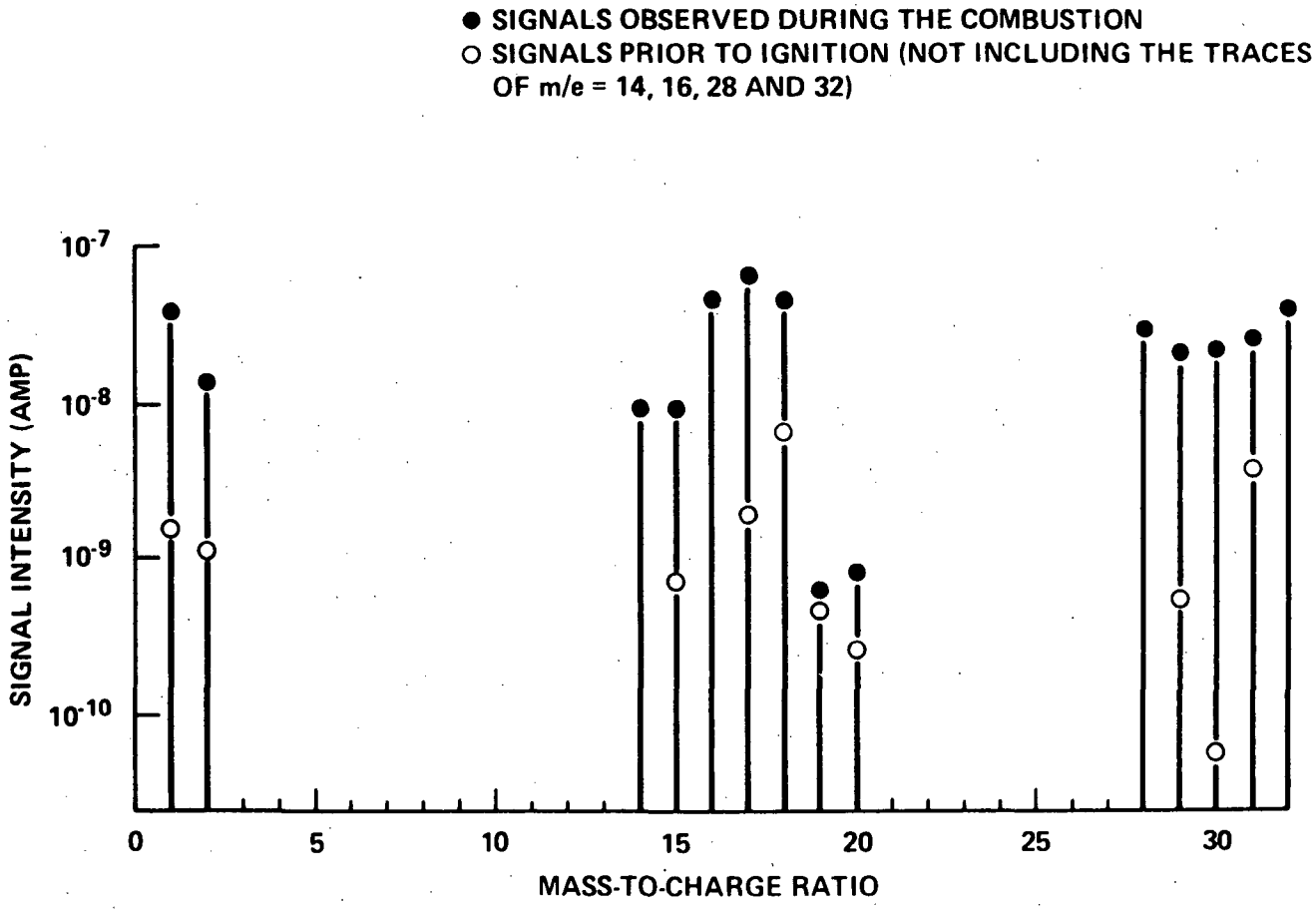

Figure 12(c). Mass Spectrum Observed at Sampling Location F1.

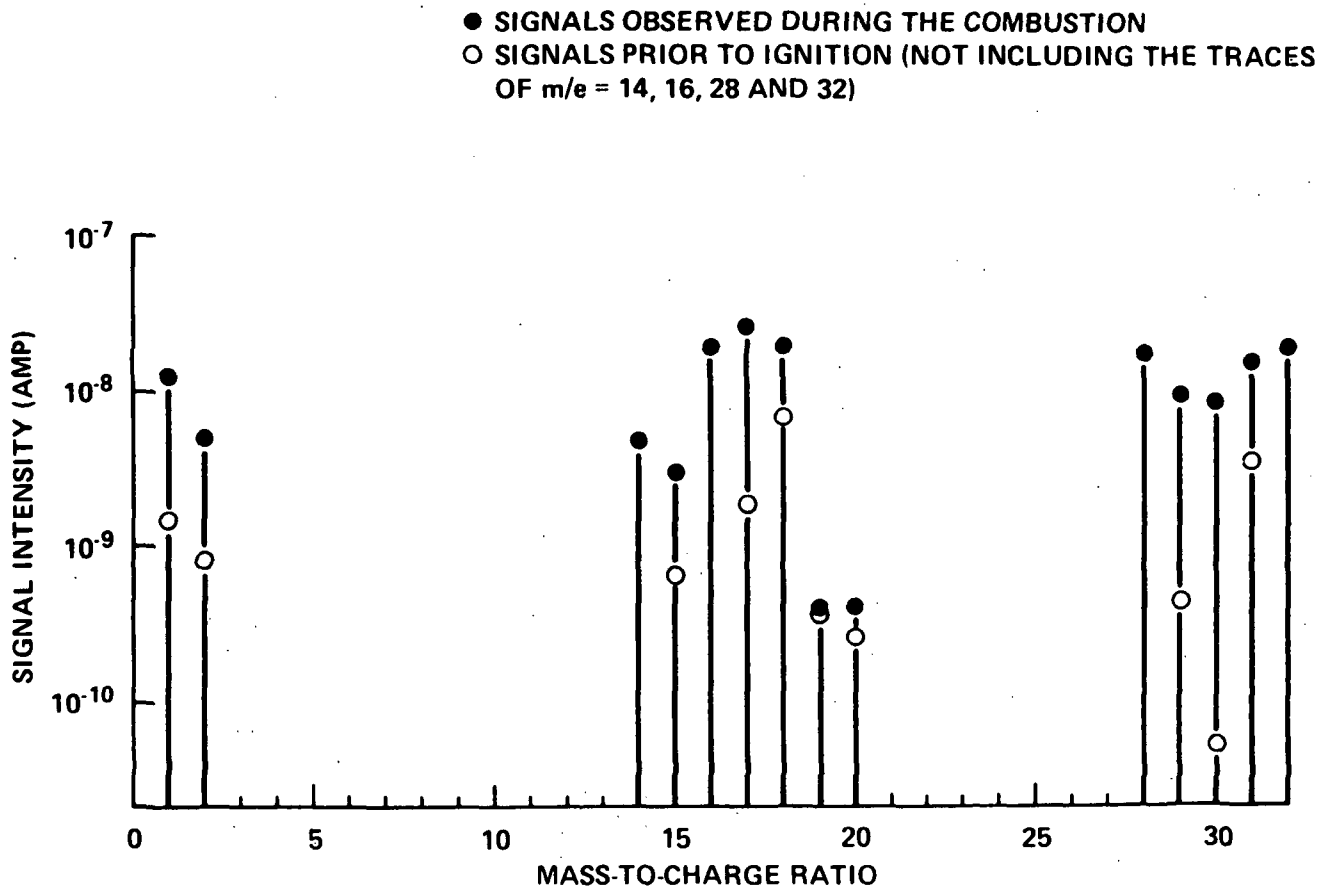

Figure 12(d). Mass Spectrum Observed at Center Sampling Location.

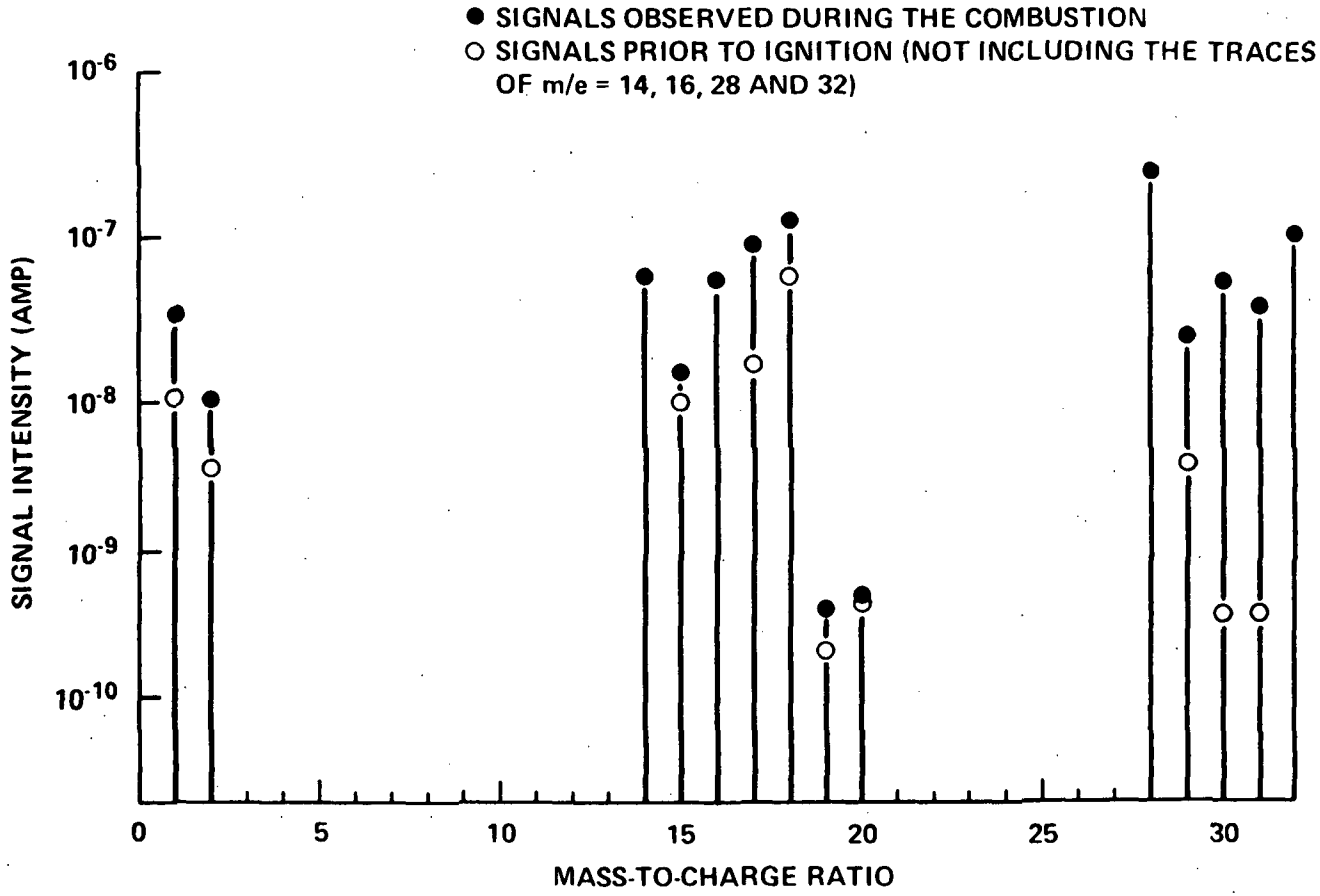

Figure 12(e). Mass Spectrum Observed at Sampling Location 01.

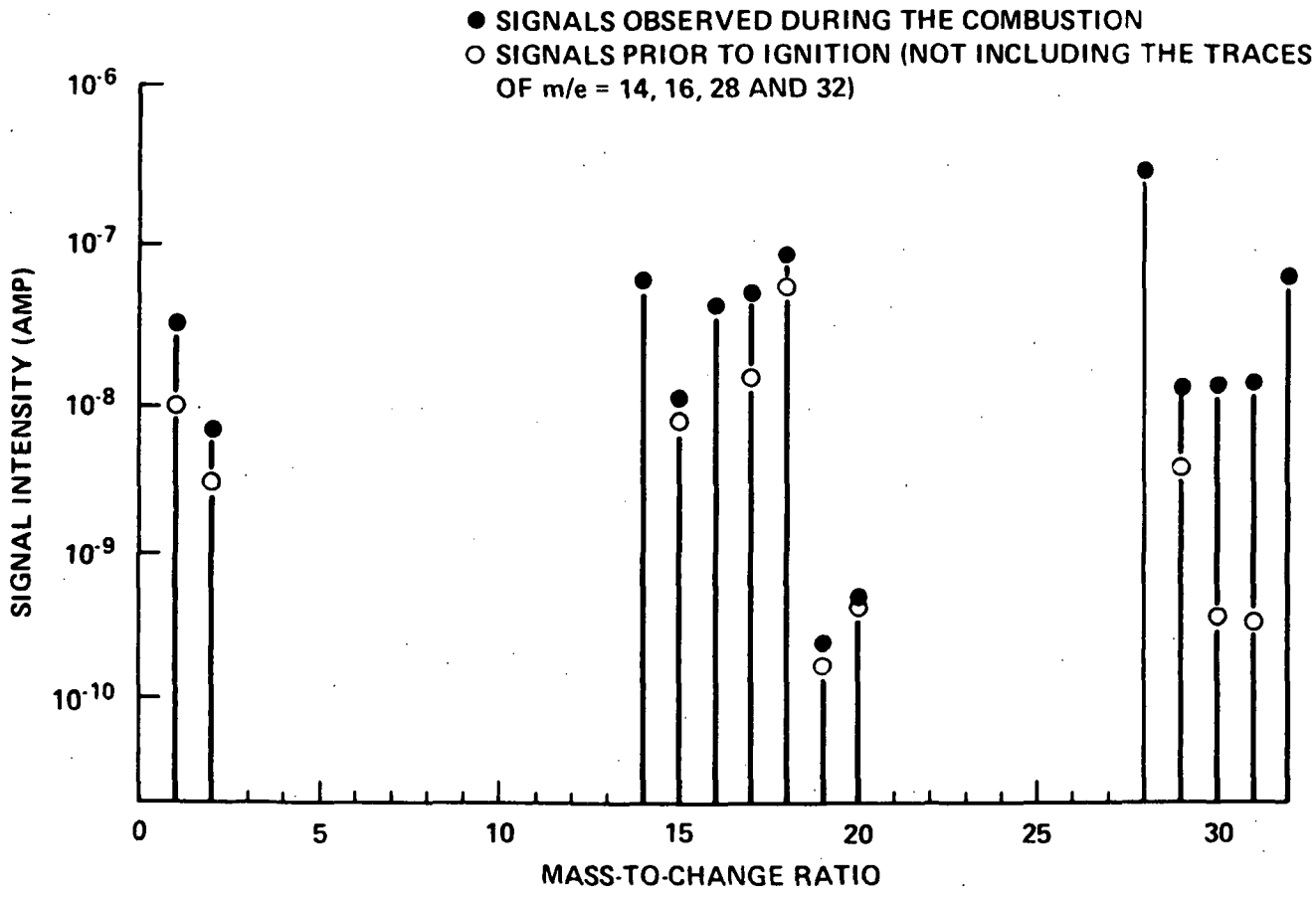

Figure 12(f). Mass Spectrum Observed at Sampling Location 02.

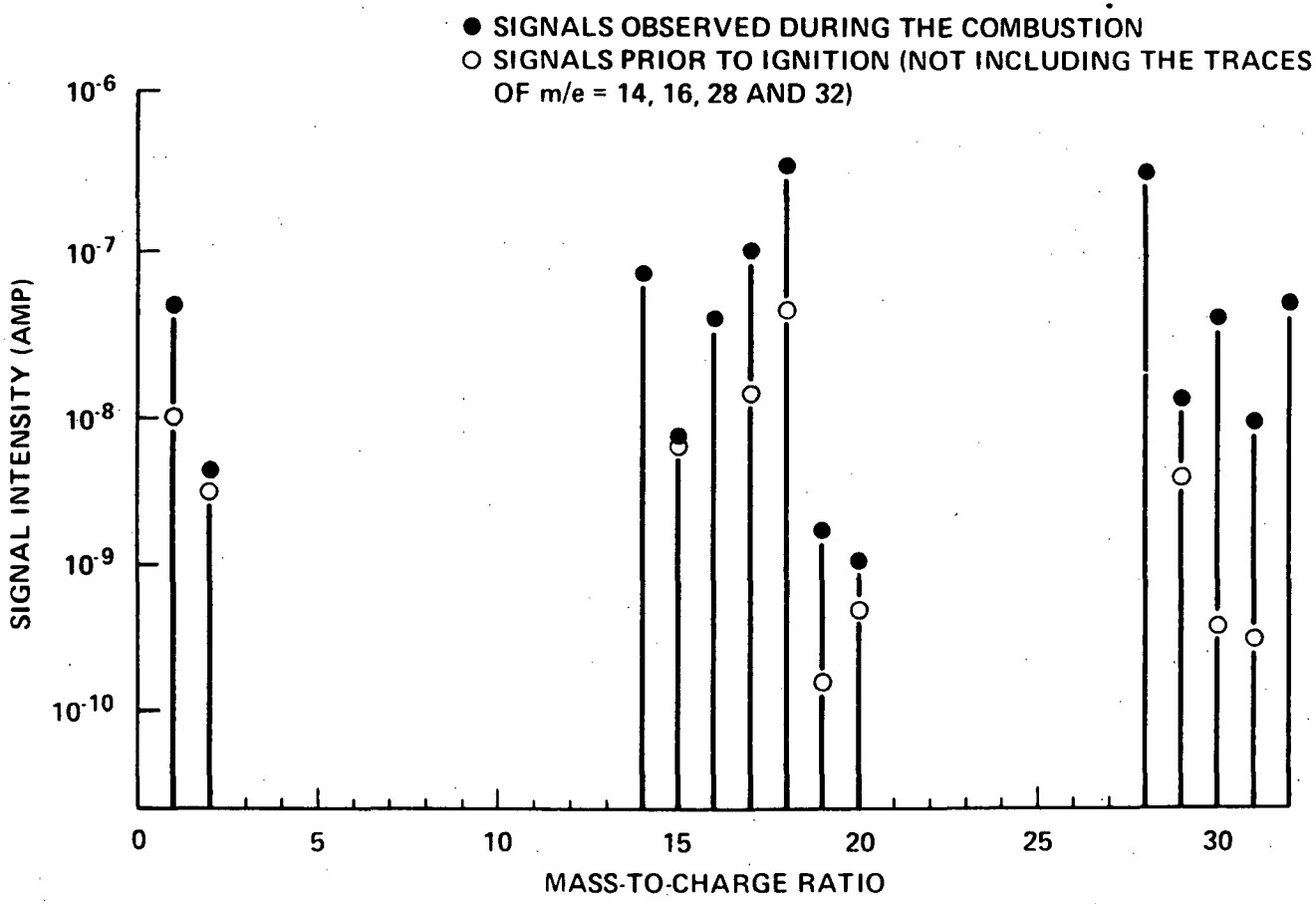

Figure 12(g). Mass Spectrum Observed at Sampling Location 03.